Int. J. Electrochem. Sci., 15 **(2020)** 2948 – 2960, doi: 10.20964/2020.04.30

International Journal of
ELECTROCHEMICAL
SCIENCE
www.electrochemsci.org

Safe Hybrid Electrolytes Based on Ionic Liquid and Carbonate Solvents for High-Temperature Li-rich Lithium-Ion Battery

Liang Dong, Cuihua Li, Fuxiao Liang, Jianhong Liu, Dong Wang, Dayong Gui, Caizhen Zhu*

College of Chemistry and Environmental Engineering, Shenzhen University, Shenzhen 518060, China
*E-mail: licuihuasz@163.com (C. Li), 2150110318@email.szu.edu.cn

Received: 5 May 2019 / *Accepted:* 1 July 2019 / *Published:* 10 March 2020

This work focuses attention on investigating N-butyl-N-methylpiperidinium bis(trifluoromethylsulfonyl) imide ($PiP_{14}TFSI$)/carbonate-based electrolytes. The main goal is to substitute a conventional $LiPF_6$/carbonate electrolyte for Li-rich/Li cells operating under both high voltage and high temperature. The safe electrolytes exhibit excellent physical and electrochemical properties at temperatures higher than 55℃. The Li-rich/Li cells with ionic liquid (IL)/fluoroethylene carbonate (FEC)-based electrolyte obtained 163.1 and 180.3 mA h g^{-1} at 0.5 C at 55℃ and 1 C at 70℃ after 100 cycles, respectively. The Li-rich/Li cell with IL/FEC-based electrolyte also achieved brilliant cyclic performance at 85℃, which is considered an extreme temperature. The remarkable cyclic performance at high temperature is ascribed to a dense and robust solid electrolyte interface (SEI) film originating from the IL/FEC-based electrolyte. According to the properties of the IL/FEC-based electrolyte, the proposed electrolyte material is promising for application to a high-temperature lithium-ion battery.

Keywords: High-temperature Li-rich cell; Safety; Ionic liquid; High voltage electrolytes; Solid-electrolyte interface

1. INTRODUCTION

Lithium-ion batteries (LIBs) can be found in different fields because these batteries are considered to have both outstanding capacity and long life-cycle. [1-3] However, safety concerns that are generated in its utilization process hinder recent development of LIBs owing to a big influence of flammable organic solvent under high voltage and temperature. [4-6] As a popular cathode material, the Li-rich cathode exhibits high operating voltage and high energy density; it also has strong cycling stability at elevated temperature according to recent reports. [7, 8] Moreover, increasing the operating temperature of LIBs is an effective method to obtain higher energy density. [9-11] Therefore, design of

an electrolyte that can withstand high voltage and temperature while being compatible with the Li-rich cathode is quite urgent.[12-14]

In addition, the actual requirements of LIBs cannot be fulfilled by conventional electrolytes consisting of lithium hexafluorophosphate ($LiPF_6$) and organic carbonate solvents. First, carbonate solvents in the conventional electrolyte limit cell operating temperatures to less than 55℃ owing to their highly volatile and flammable properties. [15] Additionally, a resistive and unstable solid electrolyte interface (SEI) film can be caused by using $LiPF_6$,[16], and the resulting HF from the decomposition product brings about dissolution of Mn and Ni ions, which results in poorer cell performance, especially in the case of high voltage and a high-temperature environment.[17] Generally, elevated temperature clearly accelerates the side reaction between electrolyte and electrodes, thus increasing the safety risk of the battery.[18]

To address the disadvantages of organic solvents, many studies have investigated extensively. Mainly researches are based on room temperature ionic liquids (RTILs), which possess properties of high thermal stability, wide electrochemical window, nonflammability, and negligible vapor pressure. [19] It is necessary and imperative for safer electrochemical energy storage devices to own these functions, and the devices include the lithium-ion battery and the sodium-ion battery, as well as supercapacitors. [20, 21] Cao et al. [22] reported that the cycling performance of RTIL/LiTFSI electrolyte is superior to the cycling performance of $LiPF_6$/carbonate-based electrolyte at elevated temperatures. Elia et al. [23] investigated enhanced IL-based electrolytes utilized in lithium-ion batteries, and exceptional long-life cycling performance was achieved at 40℃ because of a stable interface upon cycling. Böhme et al. [12] indicated that LIBs cycled with an IL-based electrolyte can operate at an elevated temperature of at least 80℃. Pure ionic liquid as the electrolyte appears to provide high thermal stability and wide electrochemical windows, but slow diffusion of Li ions and high viscosity within the electrolyte restrict the practical application. [24] In recent years, several articles reported that mixing ILs with organic solvent is a feasible way to improve the performance of the electrolyte. Ababtain et al. [25] proposed that the key for improving a safe and high-temperature lithium-ion battery is enhancing the ion transport of ionic liquid-based electrolytes without compromising thermal stability, and a systematic study revealed that the 20% propylene carbonate (PC)/IL electrolyte increased capacity significantly at 100℃ with minimal loss during cycling. Chen et al. [26] claimed that PC alone is not sufficient to form an effective SEI film, while incorporation of ethylene carbonate (EC) can significantly improve surface passivation on the electrode. Meanwhile, FEC is considered an effective SEI formation additive and is usually used as a cosolvent. Plylahan et al. [27] had shown the inclusion of organic solvent enhanced the ion transport, and electrolyte-containing FEC cycled stably at 80℃ for 300 cycles, whereas the electrolyte employing ILs as the sole matrix suffered rapid fading of capacity.

In this study, ionic liquid N-butyl-N-methylpiperidinium bis(trifluoromethylsulfonyl) imide ($PiP_{14}TFSI$) has been introduced as the main component to the electrolyte system, and PC, EC, and FEC are used as cosolvents. Lithium difluoro(oxalato) borate (LiDFOB), which possesses excellent film-forming ability even in a high-temperature environment as reported [28] is used as the Li salt. We conducted a systematic investigation on $PiP_{14}TFSI$/carbonate-based electrolytes and conventional electrolytes to compare the effects on thermal stabilities, electrochemical windows, cyclic performance

of Li-rich/Li cells at high temperature. The chemical structures of $PiP_{14}TFSI$, PC, LiDFOB, EC and FEC are presented in Figure 1.

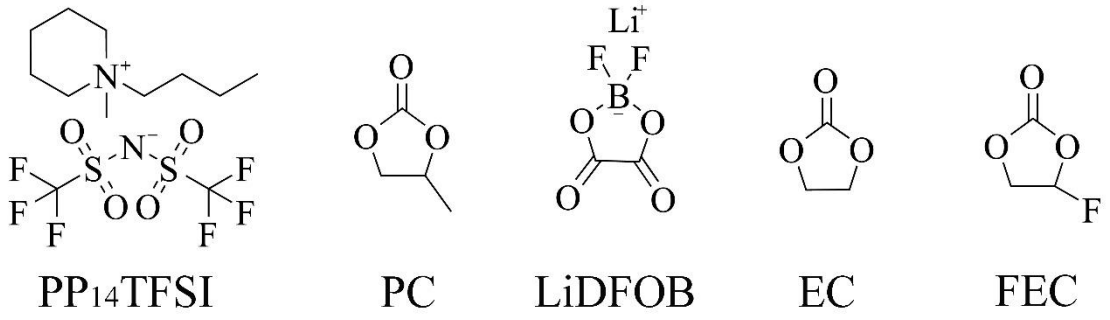

Figure 1. Structural information for components in electrolytes investigated.

2. EXPERIMENTAL

The synthetic procedure for IL is according to previous reports. [28, 29] The trace water in IL was eliminated by vacuum drying. The $PiP_{14}TFSI$/carbonate-based electrolytes were prepared using ternary solvents composed of $PiP_{14}TFSI$ (N-butyl-N-methylpiperidinium bis(trifluoromethylsulfonyl) imide), PC (propylene carbonate), EC (ethylene carbonate) or FEC (fluoroethylene carbonate), and expressed as IL/EC- and IL/FEC-based electrolytes, and LiDFOB was dissolved in mixtures with a constant concentration of 0.5 mol/kg. LiDFOB was purchased from Suzhou Fosai Inc. The detailed compositions are present in Table 1.

Table 1. The composition of the electrolytes investigated in this work.

Electrolyte	$PP_{14}TFSI$ (wt %)	PC (wt %)	EC (wt %)	FEC (wt %)	LiDFOB (mol/kg)
IL/EC	60	30	10	0	0.5
IL/FEC	60	30	0	10	0.5

To conduct comparisons, we prepared conventional electrolyte by dissolving 1 M $LiPF_6$ in a solvent (EC/DEC/EMC in 3:2:5 weight ratio), namely, the $LiPF_6$/org. Li-rich electrode is comprised of 80 wt % active material $Li_{1.15}(Ni_{0.36}Mn_{0.64})_{0.85}O_2$ (Jiangte Lidian Co. Ltd.), 10 wt % polyvinylidene fluoride (PVdF) and 10 wt % acetylene black. Each electrode contains 1.7-1.9 mg Li-rich material. Coin cells assemblages were accomplished by using Li foil, prepared electrodes and electrolytes with a polypropylene separator (Celgard), operating in the glove box (Mbraun), where H_2O and O_2 are controlled under 0.1 ppm.

The AC impedance method is adopted for the purpose of measuring the ionic conductivity in a conductive cell. Meanwhile, the conductive cell is equipped with Pt electrodes. The conductive cell was placed in a thermostated oven (FUYIDA) to control test temperature. The anodic stability of the

investigated electrolytes was determined by linear sweep voltammetry (LSV) measurement at different temperatures. The Pt electrode is utilized as the working electrode. The counter electrode and reference electrode is Li foil, scan rate is 0.1 mv/s. The assembled Li-rich/Li cells were measured on a battery test system (Land, Wuhan) to acquire cyclic performance between 2-4.6 V under different temperatures. The operating temperature is controlled by a thermostat. As to the electrochemical impedance spectra (EISs), the data were acquired on a Solartron 1470E potentiostat with FRA 1260 frequency response analyzer in a frequency range of 10^5 Hz to 0.1 Hz.

The flammability test of the electrolyte solution was performed by observation of the flame formation process on the liquid surface for a few seconds, which follows the reported procedure. [30-32] Thermogravimetric analysis (TGA) of the investigated electrolytes was realized by using a TGA analyzer (TA Q50), and the range of temperatures was 35-600℃. The heating rate was 10 K/min, and the sample remains in the N_2 atmosphere. Cycled Li-rich electrodes were retrieved by dismantlement of cells, and anhydrous dimethyl carbonate (DMC) is used to rinse the cycled cathode two times in a glove box. After drying, the surface was characterized on a JEOL scanning electron microscope (SEM). The composition of the SEI film was characterized by X-ray photoelectron spectroscopy (XPS, K-Alpha+, Thermo Fisher). The quantity of retaining metal ions in the cycled electrode is analyzed by the procedure based on our previous report. [28]

3. RESULTS AND DISCUSSION

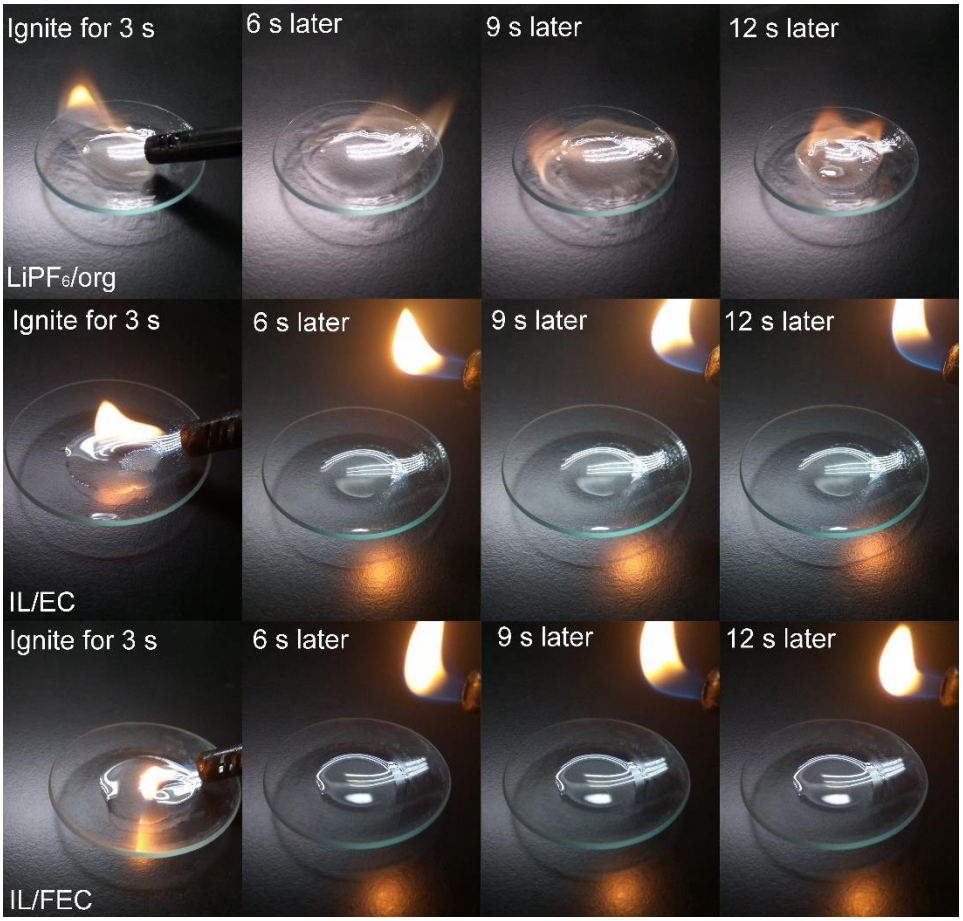

Figure 2. Flammability tests on $LiPF_6$/org, IL/EC, IL/FEC electrolytes.

Electrolyte flammability is vital in exploring the safety issue of lithium-ion battery. [33] The flammability test of investigated electrolytes was carried out for the purpose of evaluating the safety of electrolytes in a visual way. As shown in Figure 2, $LiPF_6$/org electrolyte is highly flammable and ignited easily. The lighter flame contacted the $LiPF_6$/org electrolyte and in 3 seconds, the electrolyte ignited and burned fiercely. In contrast, significantly reduced flammability was observed in case of $PiP_{14}TFSI$/carbonate-based electrolytes. IL/EC- and IL/FEC-based electrolytes did not exhibit any combustion when exposed to flame, indicating that battery safety can be improved remarkably when 60 wt % ionic liquid exists in electrolytes, and this is truly in accord with previous reports. [29]

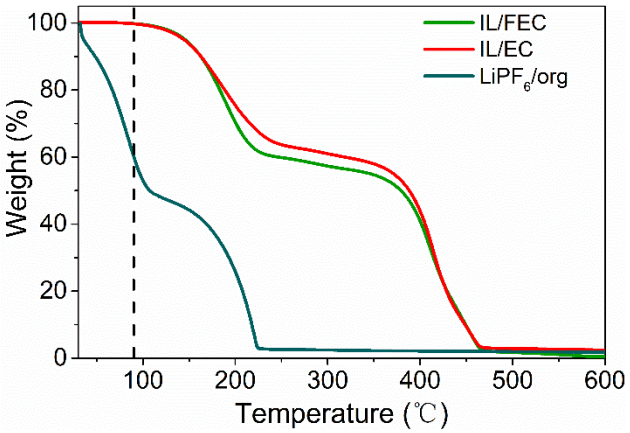

Figure 3. Thermogravimetric curves of $PP_{14}TFSI$/carbonate and $LiPF_6$/org electrolytes.

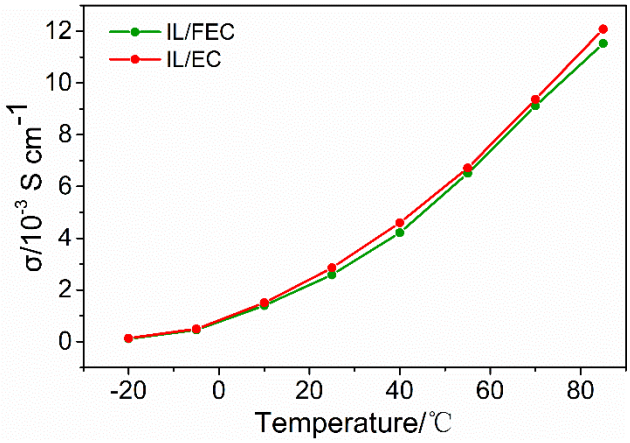

Figure 4. Ionic conductivity for IL/EC- and IL/FEC-based electrolytes from -20 to 85℃.

For a high-temperature electrolyte, thermal stability in the operating temperature range is quite essential. In this study, all considered electrolytes were investigated in a N_2 atmosphere by TGA analysis from 35℃ to 600℃. As shown in Figure 3, $LiPF_6$/org electrolyte suffered severe thermal weight loss in the given temperature range, which is ascribed to volatilization of carbonate solvents. In contrast, no obvious weight loss can be seen until 90℃ in the curves of $PiP_{14}TFSI$/carbonate-based electrolytes, and the weight loss in the range of 90℃ to 465℃ is known for volatilization of carbonate solvents and decomposition of carbonate solvents and $PiP_{14}TFSI$. According to the results, remarkable thermal

properties of $PiP_{14}TFSI$/carbonate-based electrolytes make application into high-temperature electrolyte systems possible.

Figure 4 shows the variations of $PiP_{14}TFSI$/carbonate-based electrolytes in ionic conductivity with temperature. Ionic conductivity of electrolytes depends on temperature to a great extent. Table 2 displays some detailed information regarding variation of ionic conductivity with temperature.

Table 2. Ionic conductivities of investigated electrolytes at various temperatures.

	Ionic conductivity/10^{-3} S cm^{-1}				
Electrolyte	-20℃	25℃	55℃	70℃	85℃
IL/EC	0.137	2.857	6.711	9.363	12.081
IL/FEC	0.116	2.583	6.506	9.116	11.521

The ionic conductivity of the IL/EC-based electrolyte demonstrates 2.857 mS cm^{-1} at 25℃. Finally, at 85℃, the value remains at 12.081 mS cm^{-1}. When we change EC to FEC, the IL/FEC-based electrolyte exhibits a lower value of ionic conductivity than the IL/EC-based electrolyte (0.116, 2.583 and 11.521 mS cm^{-1} at -20℃, 25℃ and 85℃, respectively), which is attributed to FEC possessing higher viscosity than EC. The similar trend was observed by Todorov et al. [34] who reported that EC is more effective than FEC in conductivity enhancement. Although the IL/EC-based electrolyte exhibits higher ionic conductivity than the IL/FEC-based electrolyte, it is difficult to say that the IL/EC-based electrolyte possesses better electrochemical performance.

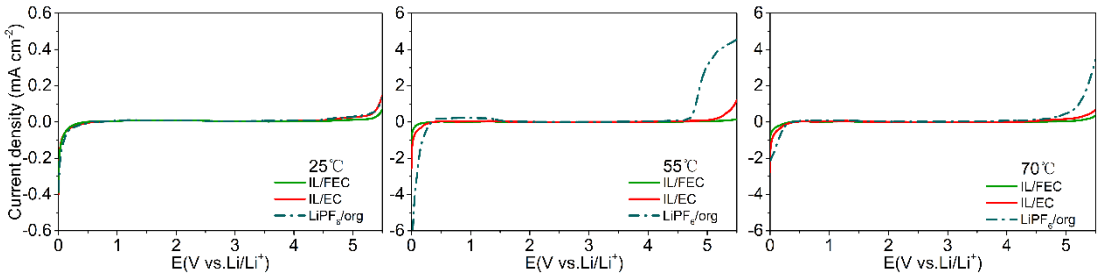

Figure 5. Linear sweep voltammetry traces of the electrolytes at 25℃, 55℃, and 70℃.

In addition, the electrolytes electrochemical window is regarded as a key factor in the process of evaluating electrochemical stability. [35] Electrochemical windows of $PiP_{14}TFSI$/carbonate-based electrolytes are depicted in Figure 5, and it is discussed by comparing the characteristics of $LiPF_6$/org electrolyte. At 25℃, oxidative stabilities that are higher than 4.6 V vs. Li/Li^+ can be presented by various electrolytes. When the temperature has reached 55℃, $LiPF_6$/org electrolyte oxidative decomposition potential can be displayed at 4.6 V vs. Li/Li^+, whereas the higher oxidation potential of $PiP_{14}TFSI$/carbonate-based electrolytes is observed, 5.0 V vs. Li/Li^+ for IL/EC-based electrolyte, 5.2 V vs. Li/Li^+ for IL/FEC-based electrolyte, which indicates that the $LiPF_6$/org electrolyte more easily

electrochemically decomposed than the $PiP_{14}TFSI$/carbonate-based electrolytes. When increasing operating temperature to 70℃, lower oxidative decomposition potential at 3.7 V vs. Li/Li^+ can be observed in curve of the $LiPF_6$/org electrolyte due to severe electrolyte decomposition at high temperature. The IL/EC-based electrolyte suffered a serious oxidative decomposition reaction above 4.6 V vs. Li/Li^+, but the IL/FEC-based electrolyte still presented a high oxidation potential of 5.0 V vs. Li/Li^+ because FEC is more electrochemically stable than EC. [36] According to these results, $PiP_{14}TFSI$/carbonate-based electrolytes seem to be practical candidates for the Li-ion battery both at high voltage and high temperature.

Nevertheless, electrochemical window identified by inert electrodes cannot directly apply to real cell conditions and materials. Hence, cyclic performance of investigated electrolytes was compared at elevated temperatures. As shown in Figure 6a, at 55℃, a severe capacity loss from 165.7 to 96.5 mA h g^{-1} cycled at 0.5 C is observed in $LiPF_6$/org electrolyte containing cell between 2 to 4.6 V, exhibiting only 58.2% capacity retention, which is consistent with our previous work. [28, 37] For the IL/EC-based electrolyte, the discharge capacity amounts to 113.9 mA h g^{-1}, 66.7% capacity retained after 100 cycles. The negative cycling performance of $LiPF_6$/org and the IL/EC-based electrolytes is attributed to low oxidation potential at elevated temperature, which leads to formation of an unstable SEI film and electrode corrosion in the high-temperature environment. However, cells cycled with the IL/FEC-based electrolyte present satisfactory cycling performance, delivering a capacity of 163.1 mA h g^{-1} with 94.3% capacity retained. When increasing the temperature to 70℃, as shown in Figure 6b, IL/FEC-containing cells obviously display a larger discharge capacity of 180.3 mA h g^{-1} at 1 C rate and preserve 81.9% capacity after 100 cycles.

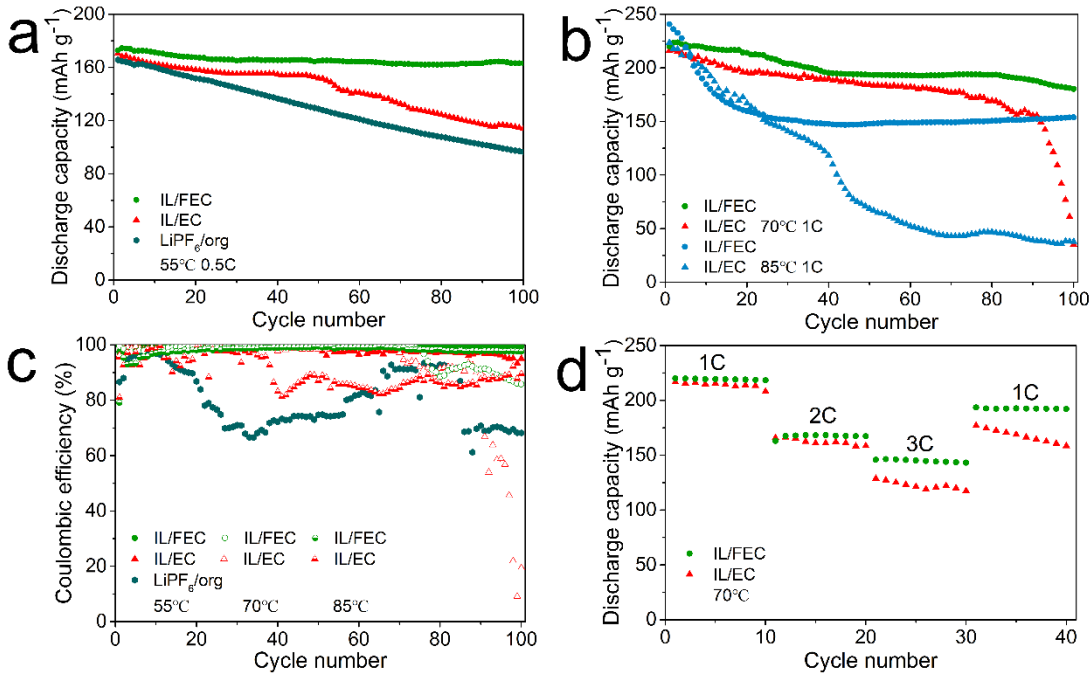

Figure 6. Cycle performance, rate capability and coulombic efficiency of investigated electrolytes in Li/Li-rich half cells at high temperatures.

The cell cycled with the IL/EC-based electrolyte at 70℃ suffered serious capacity degradation upon cycles, which originated from 216.3 to 35.2 mA h g^{-1}, with only 16.2% capacity reserved. The considerable improved electrochemical performance of IL/FEC is ascribed mainly to the formation of a more intensive and stable SEI film on the Li-rich cathode surface, which can effectively suppress polarization and protect the cathode structure, compared to the situation where the IL/EC-based electrolyte was used. More details will be discussed later. Furthermore, the discharge capacity of $PiP_{14}TFSI$/carbonate-based electrolyte at 70℃ is larger than the discharge capacity of $PiP_{14}TFSI$/carbonate-based electrolyte at 55℃. This result is due mainly to ionic conductivity being improved when the temperature is elevated. [38]

To conduct a further investigation of the cycling performance of $PiP_{14}TFSI$/carbonate-based electrolyte (especially IL/FEC), the Li-rich/Li cell was measured at 85℃. As depicted in Figure 6b, although the capacity of the IL/FEC-based electrolyte containing cell presents a capacity loss upon cycle, a significant improvement in cycling performance can be observed compared to the cell cycled with IL/EC-based electrolyte. Figure 6c exhibits the coulombic efficiency of cells cycled with all investigated electrolytes. The coulombic efficiency of the IL/FEC-based electrolyte reveals more stability than other electrolytes containing cells at 55℃, 70℃ and 85℃. Overall, the excellent cycling performance manifests that the IL/FEC-based electrolyte is a suitable candidate. Figure 6d exhibits the rate performance of IL/EC- and IL/FEC-based electrolytes containing Li-rich/Li cells. The IL/FEC-based electrolyte could reach a capacity of 146.3 mA h g^{-1} at 3 C, but the IL/EC-based electrolyte presents a lower capacity value than the IL/FEC-based electrolyte. Furthermore, when returning to the 1 C rate, the capacity derived from the IL/FEC-based electrolyte containing cell restored considerably, whereas the cell using the IL/EC-based electrolyte is only partly restored. The final results show that the IL/FEC-based electrolyte can restrain continued electrolyte decomposition and enhance Li^+ ion diffusion, thus resulting in a further improvement of the rate performance.

Table 3. Fitted values (Ω) of EISs for Li/Li-rich cells after cycles at 55℃ and 70℃.

Temperature (℃)	Sample	Before cycles	After 3 cycles	After 100 cycles	
		R_{ct}	R_{ct}	R_f	R_{ct}
55	IL/EC	125.1	138.1	81.1	149.4
55	IL/FEC	283.4	263.1	91.8	145.4
70	IL/EC	137	297.6	34.1	428.5
70	IL/FEC	258.1	249	86.1	318.2

To study the interfacial properties of Li-rich/Li cells during cycling, we adopted electrochemical impedance spectral (EIS) measurement to get a further understanding of impedance evolution of the cells. Figure 7 depicted AC impedance curves of Li-rich/Li cells at different cycles. Typically, the high

frequency part represents the resistance of the SEI film (R_f), and the middle part of the semicircle is usually attributed to resistance of charge transfer (R_{ct}). [39] An appropriate equivalent circuit is designed to fit EIS curves. Table 3 presents fitted results.

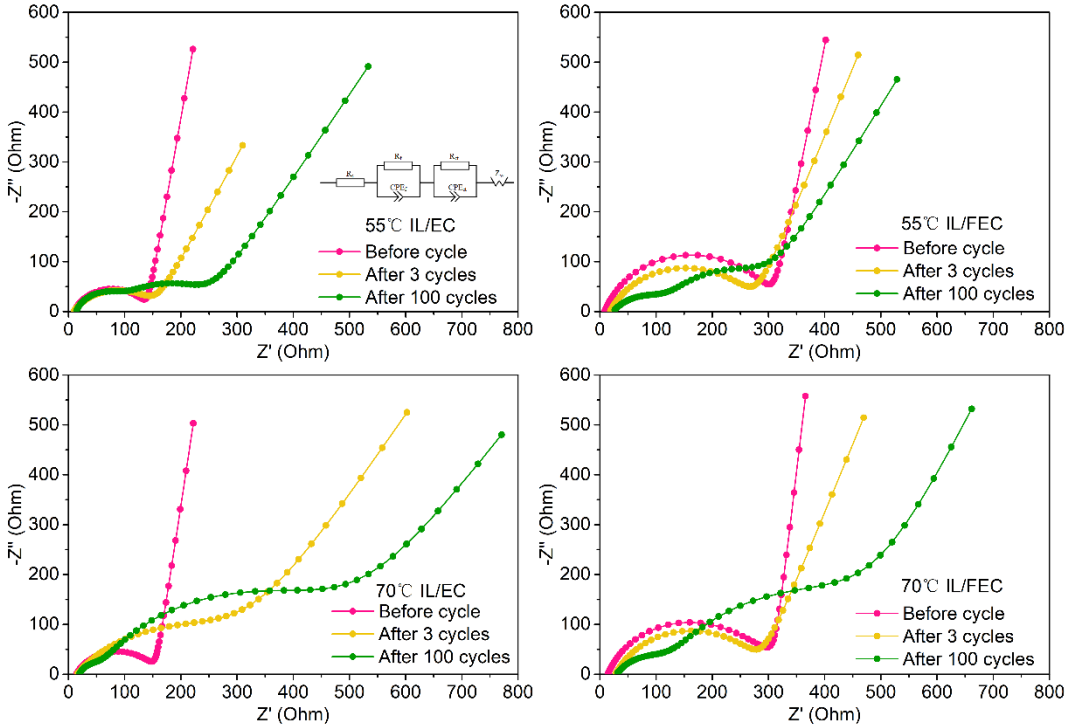

Figure 7. AC impedance curves of Li/Li-rich cell using investigated electrolytes at 55 and 70℃.

Both lower viscosity and higher wettability are widely acknowledged to perform a vital role in decreasing the impedance of the pristine cell [27, 40], so the resistance of the cell cycled with the IL/EC-based electrolyte before cycle is smaller than the resistance of the cell cycled with the IL/FEC-based electrolyte. At 55℃, the impedance of the cell cycled with the IL/EC-based electrolyte increases considerably to 149.4 Ω of R_{ct} value after 100 cycles, implying that an unstable interface film is formed during the cycling process. [41] The increasing R_{ct} impedance is ascribed to the detrimental SEI film formed by severe interfacial reaction when the IL/EC-based electrolyte is used, because the IL/EC-based electrolyte exhibits lower oxidative potential at elevated temperatures. In contrast, the R_{ct} value of the cell cycled with the IL/FEC-based electrolyte decreased to 145.4 Ω after 100 cycles, suggesting that the SEI film derived from the IL/FEC-based electrolyte is relatively more stable and compact. When elevating temperature to 70℃, the R_{ct} values of cells with IL/EC- and IL/FEC-based electrolytes increase with cycle number, but the latter electrolyte shows a slight increase, which is much lower than the cell with the IL/EC-based electrolyte. The decreased R_{ct} values reveal that a more stable SEI film is formed, thus stabilizing the interface between cathode and electrolyte at elevated temperature to ensure better cycling performance, in good accord with cycling performance results.

To observe the morphology of the SEI film, SEM images of a cycled Li-rich cathode were collected. It is easy to find some evidence of electrolyte decomposition and growth of the SEI film. Figure 8 demonstrates that the pristine Li-rich cathode possesses clean and smooth surface with spherical

particles (Figure 8a). [42] For the Li-rich electrode after cycled with the IL/EC-based electrolyte at 55℃ and 70℃ (Figure 8b and d), the surface is unpolished with severe structural decomposition, covered with the decomposition product of the electrolyte.

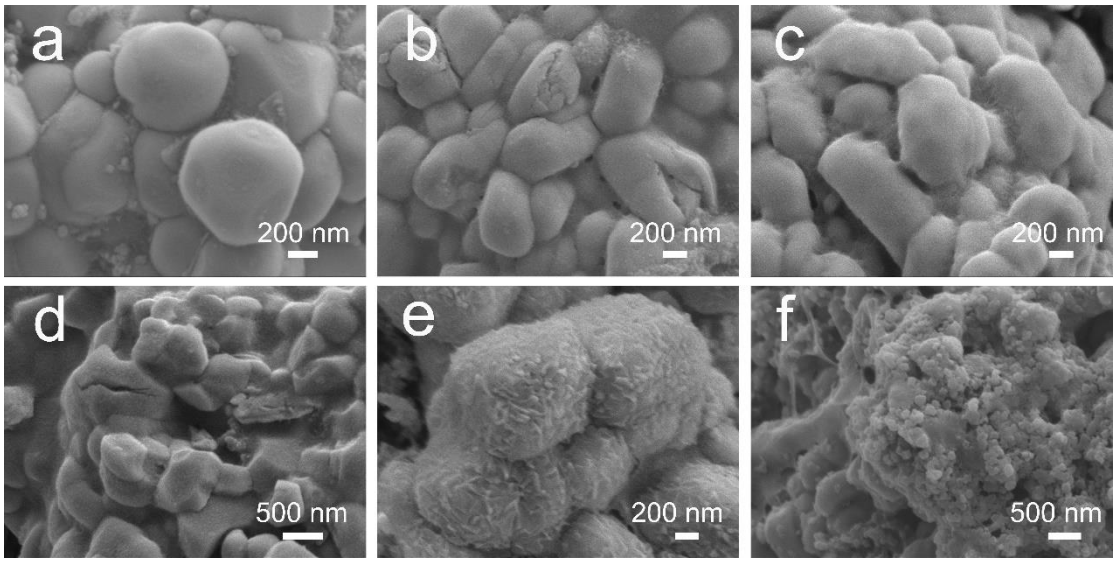

Figure 8. Morphology of pristine cathode (a), cycled Li-rich cathodes with electrolyte IL/EC (b), IL/FEC (c) at 55℃, IL/EC (d), IL/FEC (e) at 70℃ (e), IL/FEC at 85℃ (f).

Lower oxidative stability leads to unfavorable and fierce interfacial reaction at elevated temperatures, and this easily results in the increase of impedance and the fading of capacity. However, for the cathode after cycled with the IL/FEC-based electrolyte at elevated temperature, uniform and dense SEI film could be observed and covered the surface of the particles (Figure 8c and e), thus confirming structural robustness, indicating less electrolyte decomposition and interfacial reaction of IL/FEC-based electrolyte during cycling. This phenomenon is related to cyclic performance and EIS results. After cycled at the extremely high temperature of 85℃, the SEI film generated by the IL/FEC-based electrolyte is unpolished and blurry with the cathode structure partially collapsed (Figure 8f), probably due to structure stability during cycling at extremely high temperature.[8]

To probe the chemical component of the SEI film, an XPS experiment was performed on the pristine and cycled cathode with the IL/EC-based electrolyte and the IL/FEC-based electrolyte at 55℃ and 70℃. As provided in Figure 9, pristine cathode C 1s presents three peaks, where the C-C (284.9 eV) peak is characteristic of acetylene black, and the other two signals at 286.3 eV and 291.2 eV are characteristic of C-H and C-F bonds associated with PVdF. The C-F signal is also found in the F 1s spectrum. [39] A dominant peak found in the O 1s spectrum at 529.7 eV is ascribed to metal oxide (namely, metal-O), and a low quantity of Li_2CO_3 is observed, which is frequently observed on a fresh cathode surface.[43]

After the cells were cycled with IL/FEC-based electrolytes at 55℃ and 70℃, some changes were observed in the XPS spectra of the Li-rich cathode surface. C 1s and O 1s spectra have shown new signals. The peaks at 286.9 and 533.3 eV indicate that the C-O bond and the C=O bond can be confirmed by peaks at 289.7 and 532.2 eV. [44] The new peak in the F 1s spectrum is assigned to LiF (685.3 eV).

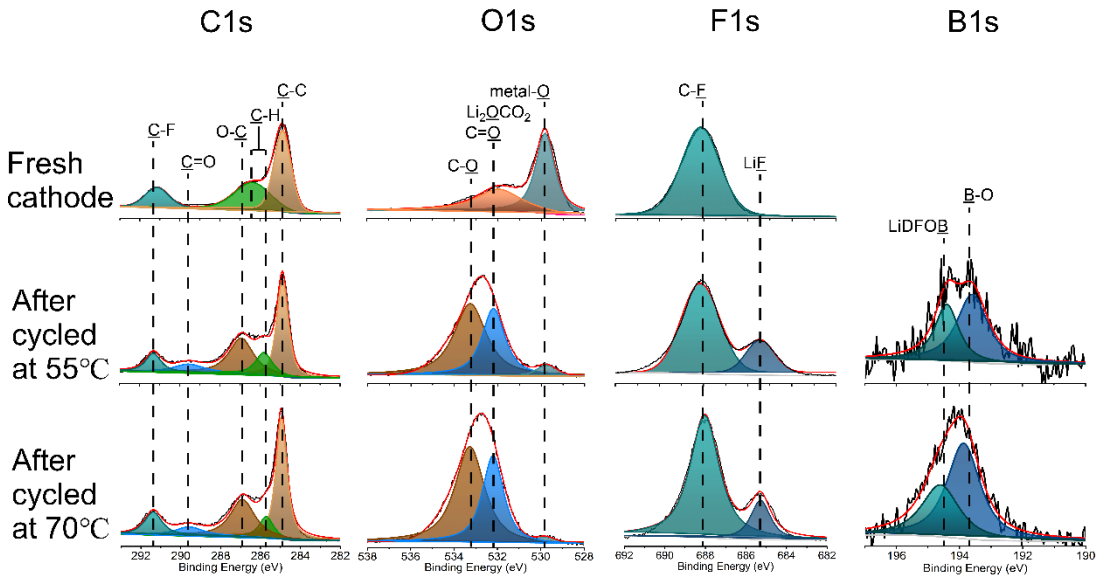

Figure 9. XPS patterns of fresh and cycled Li-rich cathode in the IL/FEC-based electrolyte at high temperatures of 55℃ and 70℃.

Signals detected in the B 1s spectrum at 193.6-193.8 eV correspond to the B-O bond, and 194.3-194.6 eV signals reveal the presence of LiDFOB. New peaks associated with new species originate mainly from the oxidative product of LiDFOB. New bond signals detected on the surface of the cathode after cycles evidence the presence of CO_2BF_2, [45] which is a main component of the SEI film. Additionally, the intensity of the new peaks observed at 70℃ is increased compared to the intensity of the new peaks observed at 55℃, suggesting that the SEI film generated at 70℃ is thicker and interfacial reaction is fiercer. This phenomenon is in accordance with impedance measurements and morphology results. Moreover, an interesting feature of the spectra is that the metal-O appears nearly invisible for the cathode after cycled at 70℃, indicating that SEI film formed is thicker than at 55℃. The dense and stable SEI film originated from the IL/FEC-based electrolyte is essential for remarkable high-temperature electrochemical performance.

To evaluate the dissolution of metal ions after cycles, residual Li, Mn, and Ni amounts in cycled cathodes were determined by ICP-AES. According to Figure 10, where the cathode in the cell containing $LiPF_6$/org and the IL/EC-based electrolyte performed at 55℃, residual Li, Mn, and Ni amounts to less than 76%, which means that severe interfacial activity occurred and leads to 24% of Li, Mn, and Ni elements being consumed, thus resulting in capacity fading and destruction of the cathode structure. With temperature increasing, more metal ions are consumed in the cell cycled with the IL/EC-based electrolyte. However, dissolution of metal ions can be effectively inhibited by the IL/FEC-based electrolyte. More than 83% and 76% of the metal ions were reserved after cycles at 70℃ and 85℃, respectively, which is ascribed to a dense and stable SEI film derived from the IL/FEC-based electrolyte formed on Li-rich particles. Hence, the SEI film formed by the IL/FEC-based electrolyte effectively inhibits metal ion loss during cycling at elevated temperatures. Therefore, the cathode material structure is maintained, which is in accord with surface characterization results.

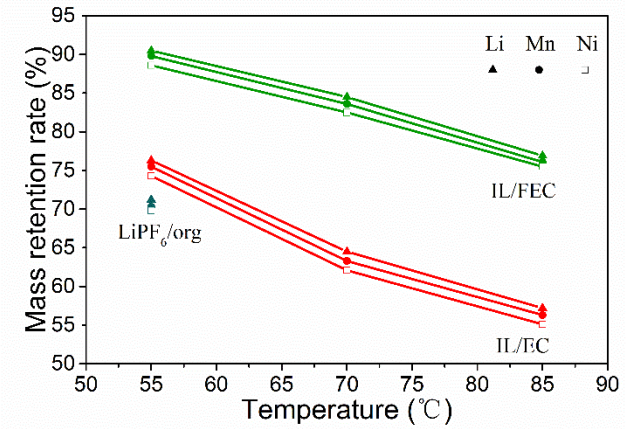

Figure 10. Retained metal ion rate in cycled Li-rich cathode with investigated electrolytes at high temperatures.

4. CONCLUSIONS

We prepared safe IL/PC/FEC ternary electrolytes that can be utilized in both high temperature and high voltage environments by combining $PiP_{14}TFSI$, PC, FEC, and LiDFOB for the Li-rich/Li cell. The nonflammability property and brilliant thermal stability reveal the high safety of the IL/FEC-based electrolyte. The IL/FEC-based electrolyte demonstrates higher oxidative potential at high temperature, compared with IL/EC and conventional electrolytes. Thanks to the SEI film formed by the IL/FEC-based electrolyte, excellent cyclic performance was achieved. The cells containing IL/FEC electrolyte retained 94.3% capacity at 55℃, and 81.9% capacity was reserved at 70℃. The robust SEI film effectively protects the cathode material structure from being destroyed and suppresses Li^+ loss. Furthermore, impedance measurements and morphology results evidence the reduced resistance and robustness properties of the interfacial film. We believe that the IL/FEC-based electrolyte possesses favorable prospects for the Li-rich lithium-ion battery at both high voltage and high temperatures.

References

1. J.B. Goodenough, Y. Kim, *Chem. Mater*., 22 (2010) 587.
2. B. Scrosati, J. Hassoun, Y.-K. Sun, *Energy & Environmental Science*, 4 (2011) 3287.
3. Y.K. Sun, S.T. Myung, B.C. Park, J. Prakash, I. Belharouak, K. Amine, *Nat Mater,* 8 (2009) 320.
4. N.-S. Choi, J.-G. Han, S.-Y. Ha, I. Park, C.-K. Back, *RSC Advances*, 5 (2015) 2732.
5. S. Tan, Y.J. Ji, Z.R. Zhang, Y. Yang, *Chemphyschem*, 15 (2014) 1956.
6. M.M. Thackeray, C. Wolverton, E.D. Isaacs, *Energy & Environmental Science*, 5 (2012) 7854.
7. P.K. Nayak, J. Grinblat, E. Levi, B. Markovsky, D. Aurbach, *J. Power Sources*, 318 (2016) 9.
8. Z. Peng, Y. Li, K. Du, Y. Cao, G. Hu, *J. Alloys Compd.*, 728 (2017) 1209.
9. J. Lin, D. Mu, Y. Jin, B. Wu, Y. Ma, F. Wu, *J. Power Sources*, 230 (2013) 76.
10. Z. Wu, X. Han, J. Zheng, Y. Wei, R. Qiao, F. Shen, J. Dai, L. Hu, K. Xu, Y. Lin, W. Yang, F. Pan, *Nano Lett.*, 14 (2014) 4700.
11. X. Xiang, X. Li, W. Li, *J. Power Sources*, 230 (2013) 89.
12. S. Böhme, M. Kerner, J. Scheers, P. Johansson, K. Edström, L. Nyholm, *J. Electrochem. Soc.*, 164 (2017) A701.
13. H. Duncan, D. Duguay, Y. Abu-Lebdeh, I.J. Davidson, *J. Electrochem. Soc.*, 158 (2011) A537.
14. K. Xu, S. Zhang, T.R. Jow, W. Xu, C.A. Angell, *Electrochem. Solid-State Lett.*, 5 (2002) A26.

15. Y.L. Kai Liu, Dingchang Lin, Allen Pei and Yi Cui, *Science Advances*, 4 (2018) 1.
16. D. Lu, M. Xu, L. Zhou, A. Garsuch, B.L. Lucht, *J. Electrochem. Soc.*, 160 (2013) A3138.
17. S.F. Lux, I.T. Lucas, E. Pollak, S. Passerini, M. Winter, R. Kostecki, *Electrochem. Commun.*, 14 (2012) 47.
18. N.P.W. Pieczonka, L. Yang, M.P. Balogh, B.R. Powell, K. Chemelewski, A. Manthiram, S.A. Krachkovskiy, G.R. Goward, M. Liu, J.-H. Kim, *The Journal of Physical Chemistry* C, 117 (2013) 22603.
19. A. Eftekhari, Y. Liu, P. Chen, *J. Power Sources*, 334 (2016) 221.
20. T. Lé, P. Gentile, G. Bidan, D. Aradilla, *Electrochim. Acta*, 254 (2017) 368.
21. C.-Y. Li, J. Patra, C.-H. Yang, C.-M. Tseng, S.B. Majumder, Q.-F. Dong, J.-K. Chang, *ACS Sustainable Chemistry & Engineering*, 5 (2017) 8269.
22. X. Cao, X. He, J. Wang, H. Liu, S. Roser, B.R. Rad, M. Evertz, B. Streipert, J. Li, R. Wagner, M. Winter, I. Cekic-Laskovic, *ACS Appl Mater Interfaces*, 8 (2016) 25971.
23. G.A. Elia, U. Ulissi, S. Jeong, S. Passerini, J. Hassoun, *Energy & Environmental Science*, 9 (2016) 3210.
24. A. Balducci, *Top Curr Chem (Cham)*, 375 (2017) 20.
25. K. Ababtain, G. Babu, X. Lin, M.T. Rodrigues, H. Gullapalli, P.M. Ajayan, M.W. Grinstaff, L.M. Arava, *ACS Appl Mater Interfaces*, 8 (2016) 15242.
26. H.-C. Chen, J. Patra, S.-W. Lee, C.-J. Tseng, T.-Y. Wu, M.-H. Lin, J.-K. Chang, *Journal of Materials Chemistry* A, 5 (2017) 13776.
27. N. Plylahan, M. Kerner, D.-H. Lim, A. Matic, P. Johansson, *Electrochim. Acta*, 216 (2016) 24.
28. L. Dong, F. Liang, D. Wang, C. Zhu, J. Liu, D. Gui, C. Li, *Electrochim. Acta*, 270 (2018) 426.
29. B. Yang, C. Li, J. Zhou, J. Liu, Q. Zhang, *Electrochim. Acta*, 148 (2014) 39.
30. A. Guerfi, M. Dontigny, P. Charest, M. Petitclerc, M. Lagacé, A. Vijh, K. Zaghib, *J. Power Sources*, 195 (2010) 845.
31. S.F. I. Quinzeni, E. Quartarone, C. Tomasi, M. Fagnoni, P. Mustarelli, *J. Power Sources*, 237 (2013) 204.
32. P. Shi, S. Fang, J. Huang, D. Luo, L. Yang, S.-i. Hirano, *Journal of Materials Chemistry A*, 5 (2017) 19982.
33. C. Arbizzani, G. Gabrielli, M. Mastragostino, *J. Power Sources*, 196 (2011) 4801.
34. Y.M. Todorov, M. Aoki, H. Mimura, K. Fujii, N. Yoshimoto, M. Morita, *J. Power Sources*, 332 (2016) 322.
35. R. Chen, Y. Chen, L. Zhu, Q. Zhu, F. Wu, L. Li, *Journal of Materials Chemistry* A, 3 (2015) 6366.
36. M. He, L. Hu, Z. Xue, C.C. Su, P. Redfern, L.A. Curtiss, B. Polzin, A. von Cresce, K. Xu, Z. Zhang, *J. Electrochem. Soc.*, 162 (2015) A1725.
37. J. Chen, Y. Gao, C. Li, H. Zhang, J. Liu, Q. Zhang, *Electrochim. Acta*, 178 (2015) 127.
38. J. Xiang, F. Wu, R. Chen, L. Li, H. Yu, *J. Power Sources*, 233 (2013) 115.
39. J. Chen, H. Zhang, M. Wang, J. Liu, C. Li, P. Zhang, *J. Power Sources*, 303 (2016) 41.
40. L. Liao, P. Zuo, Y. Ma, Y. An, G. Yin, Y. Gao, *Electrochim. Acta*, 74 (2012) 260.
41. X.-Q. Zhang, X.-B. Cheng, X. Chen, C. Yan, Q. Zhang, *Adv. Funct. Mater.*, 27 (2017) 1605989.
42. X. Li, M. Xu, Y. Chen, B.L. Lucht, *J. Power Sources*, 248 (2014) 1077.
43. M. Xu, N. Tsiouvaras, A. Garsuch, H.A. Gasteiger, B.L. Lucht, *The Journal of Physical Chemistry* C, 118 (2014) 7363.
44. M. Nie, B.L. Lucht, *J. Electrochem. Soc.*, 161 (2014) A1001.
45. F. Wu, Q. Zhu, R. Chen, N. Chen, Y. Chen, L. Li, *Nano Energy*, 13 (2015) 546.